

Intrinsic Polarized Strangeness and Λ^0 Polarization in Deep-Inelastic Production

John Ellis¹, Aram Kotzinian^{2,3}, and Dmitry V. Naumov³

¹ CERN, Geneva, Switzerland

² Yerevan Physics Institute, 375036, Yerevan, Armenia

³ JINR, Dubna, 141980, Russia

hep-ph/0204206, CERN-TH/2002-080

Abstract. We propose a model for the longitudinal polarization of Λ^0 baryons produced in deep-inelastic lepton scattering at any x_F , based on static $SU(6)$ quark-diquark wave functions and polarized intrinsic strangeness in the nucleon associated with individual valence quarks. Free parameters of the model are fixed by fitting NOMAD data on the longitudinal polarization of Λ^0 hyperons in neutrino collisions. Our model correctly reproduces the observed dependences of Λ^0 polarization on the kinematic variables. Within the context of our model, the NOMAD data imply that the intrinsic strangeness associated with a valence quark has anticorrelated polarization. We also compare our model predictions with results from the HERMES and E665 experiments using charged leptons. Predictions of our model for the COMPASS experiment are also presented.

PACS. 13.10.+q Weak and electromagnetic interactions of leptons – 13.15.+g Neutrino interactions – 13.60. r Photon and charged-lepton interactions with hadrons – 13.60.Rj Baryon production – 13.85.Hd Inelastic scattering: many-particle final states – 25.70.Mn Projectile and target fragmentation

1 Introduction

The spin structure of hadrons is still not understood at a fundamental level in QCD, despite having been extensively studied both theoretically and experimentally over

past two decades. The trigger for many of these activities was the so-called *spin crisis*, namely an unexpectedly small net quark contribution to the total spin of the nucleon: 0.27 ± 0.04 at $Q^2 = 10$ GeV 2 , reported initially by

the EMC Collaboration [1], and subsequently confirmed by a number of other experiments [2,3,4,5]. Defining Δq to be the net polarization of a given quark species q , and likewise $\Delta \bar{q}$ for the corresponding antiquarks, it has been found that:

$$\begin{aligned}\Delta u + \Delta \bar{u} &= 0.82 \pm 0.03, \\ \Delta d + \Delta \bar{d} &= -0.44 \pm 0.03, \\ \Delta s + \Delta \bar{s} &= -0.11 \pm 0.03.\end{aligned}\tag{1}$$

This result indicates the presence of strange sea quarks with negative net polarization, though the interpretation depends strongly on the gluon contribution to the nucleon spin [6]. Among the many questions still challenging both theoretical and experimental efforts we may mention:

- Are strange quarks in the nucleon indeed polarized as suggested by the deep-inelastic scattering (DIS) data?
- What is the gluon contribution to the nucleon spin?
- What is the spin content of other baryons?

There are several ongoing experimental activities dedicated to investigating the gluon contribution to the nucleon spin [3,5,7]. In principle, it is possible to measure Δs , $\Delta \bar{s}$ directly in an experiment with neutrino and anti-neutrino charged-current (CC) and neutral-current (NC) (quasi) elastic scattering off neutrons and protons [8] and in DIS from a polarized target [9]. However, for the moment there are no approved experiments of this type. Therefore, it is of great interest to have estimates of the polarization of the strange quarks in the nucleon using indirect measurements.

Using a model of polarized intrinsic strangeness [10] it was suggested [11] that strange quark polarization could manifest itself via the polarization of Λ^0 hyperons produced in the target fragmentation region of lepton-nucleon DIS along an axis that is longitudinal with respect to the momentum of the exchanged boson. Several experimental measurements of Λ^0 polarization have been made in neutrino and anti-neutrino DIS. Longitudinal polarization of Λ^0 hyperons was first observed in bubble chamber (anti) neutrino experiments [12,13,14], with the results shown in Table 1. The observed longitudinal polarization of Λ^0 hyperons varied from -0.29 ± 0.18 to -0.63 ± 0.13 , increasing in absolute value in the region $x_F < 0$. However, all these early experiments suffered from a lack of statistics, and the results could not be considered conclusive, although they were very suggestive.

The NOMAD Collaboration has recently published new and interesting results on Λ^0 and $\bar{\Lambda}^0$ polarization with much larger statistics [15,16,17]. The observed longitudinal polarization of Λ^0 hyperons produced in neutrino DIS from an isoscalar target was $P_{\Lambda^0} = -0.15 \pm 0.03(\text{stat.})$, again increasing in absolute value when $x_F < 0$: $P_{\Lambda^0}(x_F < 0) = -0.21 \pm 0.04(\text{stat.})$.

There have been a few attempts in the literature to describe Λ^0 and $\bar{\Lambda}^0$ polarization in the target fragmentation region. The polarized intrinsic strangeness model [11] mentioned earlier predicted a negative sign for the longitudinal polarization of Λ^0 and $\bar{\Lambda}^0$ hyperons. The polarization of Λ^0 hyperons in the target fragmentation region of DIS has also been considered in the meson cloud model [18].

Due to the pseudoscalar nature of the $NK\Lambda^0$ coupling, the polarization of final-state Λ^0 hyperons was predicted to be strongly anticorrelated to that of the nucleon, vanishing for an unpolarized target.

In addition to studies of the nucleon's intrinsic strangeness content, the self-analyzing properties of Λ^0 and $\bar{\Lambda}^0$ decays are crucial for investigations of the spin structure of these hadrons in experiments with a source of polarized fragmenting quarks. The possible correlation of the polarizations of the scattered quark and the final-state hadron is described by the spin transfer coefficient:

$$C_q^h(z) \equiv \Delta D_q^h(z)/D_q^h(z), \quad (2)$$

where $D_q^h(z)$ and $\Delta D_q^h(z)$ are unpolarized and polarized fragmentation functions for the quark q to yield a hadron h with a fraction z of the quark energy. We recall that Λ^0 and $\bar{\Lambda}^0$ polarization has been, or is planned to be measured in several different processes where the fragmentation of polarized quarks can be measured:

- in e^+e^- annihilation at the Z^0 pole at LEP [19],
- in polarized charged-lepton DIS off a target nucleon [7, 20, 21],
- in (anti) neutrino DIS off a target nucleon [12, 13, 14, 15, 16, 17].

These processes have been extensively studied in different theoretical models [22, 23, 24, 25, 26, 27, 28, 29, 30], in attempts to understand the spin structure of final-state hadron. The model used in this paper is described in Section 2.4, and spin effects in the quark fragmentation process. A key assumption, adopted widely, is that the struck quark fragmentation can be disentangled from the nucleon remnant

fragmentation by imposing a cut: $x_F > 0$. We discuss in Sec. 2.4 the validity of this assumption, which is important also for attempts to probe intrinsic strangeness.

It is important to recall that a significant fraction of Λ^0 hyperons are produced via decays of heavier strange particles, such as Σ^0 , Σ^* and Ξ . As was first pointed by Bigi [31], in polarized lepton-nucleon DIS these heavy hyperons may inherit polarization from the remnant diquark left behind when the struck quark is removed, or from the polarization of the fragmenting quark. The Λ^0 hyperons originating from decays of these hyperons will then also acquire some polarization, and this effect should be taken into account in any theoretical consideration.

We formulate in Section 2.1 of this paper a refinement of the polarized intrinsic strangeness model [10, 11], in which $s - \bar{s}$ pairs are associated with individual valence quarks. The intrinsic strange quarks and antiquarks may then have polarizations that are (anti) correlated with the valence quark polarizations, rather than with that of the nucleon as a whole. We assume that the valence quark wave functions are described by non-relativistic $SU(6)$ wave functions. In Section 2.2 we use this model to calculate the polarizations of Λ^0 hyperons produced promptly or via the decays of heavier hadrons from fragmentation of the remnant diquark, and in Section 2.3 we calculate the effect of struck quark fragmentation. The fragmentation

and we fix free parameters of our model from a fit to the NOMAD data. In Section 3 we present the model predictions for the polarization of Λ^0 hyperons. Those produced

in (anti) neutrino DIS are discussed in Section 3.1 and those in charged-lepton DIS are discussed in Section 3.2. Wherever possible, these predictions are compared with available data. Finally, in Section 4 we draw our conclusions.

2 Model for Λ^0 Polarization

2.1 Polarized Intrinsic Strangeness Model

The main idea of the polarized intrinsic strangeness model applied to semi-inclusive DIS is that the polarization of s quarks and \bar{s} antiquarks in the hidden strangeness component of the nucleon wave function should be (anti)correlated with that of the struck quark. This correlation is described by the spin correlation coefficients C_{sq}

$$P_s = C_{sq} P_q, \quad (3)$$

where P_q and P_s are the polarizations of the initial struck (anti)quark and remnant s quark.

Such a correlation can be motivated by a strong attraction between quark and antiquark in the spin-singlet pseudoscalar $J^P = 0^-$ channel, and the fact that vacuum quark-antiquark pairs must be in a relative spin-triplet 3P_0 state. In the original version of this model [10,11], the spin projection of the $\bar{s}s$ pair on the direction of the struck quark spin was taken to be $S_z(\bar{s}s) = -1$, *i.e.*, maximal anticorrelation between the polarizations of the struck quark and the remnant s quark was assumed, corresponding to a spin correlation coefficient $C_{sq} = -1$. However, other values of C_{sq} are also conceivable. For example, an

alternative scenario for polarized intrinsic strangeness in which the $S_z(\bar{s}s) = -1$ and $S_z(\bar{s}s) = 0$ states of the $\bar{s}s$ -pair are equally probable has been considered in [9,38]. In that case, one would have $C_{sq} = -\frac{1}{3}$. Moreover, the spin correlation coefficients could in principle be different for scattering off a valence and a sea quark: ($C_{sq_{val}} \neq C_{sq_{sea}}$).

In this paper we refine the polarized intrinsic strangeness model [10,11] as follows:

- We leave $C_{sq_{val}}$ and $C_{sq_{sea}}$ as free parameters, that are fixed in a fit to the NOMAD data [15].
- We take into account the polarization transfer from heavier hyperons.

2.2 Polarization of Strange Hadrons in Diquark Fragmentation

After removing a polarized scattered quark from an unpolarized nucleon, the remnant diquark may combine with an s quark - which could originate from the nucleon sea or from a colour string between the diquark and the scattered quark - to form a strange baryon Y . This baryon could be a Λ^0 hyperon - which we term *prompt* production - or a heavier hyperon that decays subsequently into a Λ^0 . Polarization transfer to a promptly-produced Λ^0 in νn charged-current DIS is shown in Fig. 1. In general, the strange baryon Y may inherit polarization from the spin configuration of the remnant diquark and/or the possible polarization of the strange quark.

We calculate the polarization of Λ^0 hyperons assuming the combination of a non-relativistic $SU(6)$ quark-diquark wave function and the polarized intrinsic strangeness model

described above. Specifically, we use the usual spin-flavor $SU(6)$ wave functions of octet and decuplet baryons and (3) to model the strange quark polarization.

We define the quantization axis along the three-momentum vector of the exchanged boson. The longitudinal polarization of Λ^0 hyperons produced via the $l^\uparrow N \rightarrow l'Y(J, M)X$ process, where the strange baryon $Y(J, M)$ has total spin J and third component M , is given in the target fragmentation region by:

$$P_{\Lambda^0}^{lq}(Y; N) = \frac{P_q \cdot \sum_M P_s(Y(J, M)) |\langle Y(J, M) | N \ominus q \rangle \otimes | s_{pol} \rangle|^2}{\sum_M |\langle Y(J, M) | N \ominus q \rangle \otimes | s_{pol} \rangle|^2}, \quad (4)$$

where P_q is the polarization of the struck quark, $P_s(Y(J, M))$ is the polarization of the strange quark in the baryon Y with spin state $|Y(J, M)\rangle$, and $|N \ominus q\rangle \otimes |s_{pol}\rangle$ is the combined wave function of the remnant diquark and of the s quark with longitudinal polarization C_{sq} .

In (4), we have taken into account the fact that, in both the electromagnetic decay of the Σ^0 and the strong decay of the Σ^* to Λ^0 , the non-strange diquark changes its spin from 1 to 0, while the strange quark retains its polarization [30].

After some straightforward algebra, we obtain the following predictions of non-zero polarization for Λ hyperons, where more details can be found in Appendix B:

$$P_{\Lambda}^{\nu d}(\text{prompt}; N) = P_{\Lambda}^{\bar{\nu} u}(\text{prompt}; N) = P_{\Lambda}^{l u}(\text{prompt}; N) = P_{\Lambda}^{l d}(\text{prompt}; N) = C_{sq} \cdot P_q,$$

$$\begin{aligned} P_{\Lambda}^{\nu d}(\Sigma^0; n) &= P_{\Lambda}^{\bar{\nu} u}(\Sigma^0; p) = \\ P_{\Lambda}^{l u}(\Sigma^0; p) &= P_{\Lambda}^{l d}(\Sigma^0; n) = \frac{1}{3} \cdot \frac{2 + C_{sq}}{3 + 2C_{sq}} \cdot P_q, \end{aligned} \quad (5)$$

$$\begin{aligned} P_{\Lambda}^{\nu d}(\Sigma^{*0}; n) &= P_{\Lambda}^{\nu d}(\Sigma^{*+}; p) = \\ P_{\Lambda}^{\bar{\nu} u}(\Sigma^{*0}; p) &= P_{\Lambda}^{\bar{\nu} u}(\Sigma^{*+}; n) = \\ P_{\Lambda}^{l u}(\Sigma^{*0}; p) &= P_{\Lambda}^{l d}(\Sigma^{*0}; n) = \\ P_{\Lambda}^{l d}(\Sigma^{*+}; p) &= P_{\Lambda}^{l u}(\Sigma^{*-}; n) = -\frac{5}{3} \cdot \frac{1 - C_{sq}}{3 - C_{sq}} \cdot P_q. \end{aligned}$$

In these expressions, l stands for either the charged lepton in an electromagnetic interaction or the (anti)neutrino in a neutral-current interaction. The interacting quark polarization, denoted by P_q in (5), is different in different processes, and depends in general on the quark flavour. The polarization of the interacting quark (d and u) for (anti)neutrino interactions via both charged and neutral current and for charged-lepton interactions via the electromagnetic current is shown in Table 2. In this Table, $\xi \equiv 2/3 \sin^2 \theta_W$, P_B is the charged-lepton longitudinal polarization, and $D(y) = \frac{1-(1-y)^2}{1+(1-y)^2}$ is the virtual photon depolarization factor, while y represents the relative energy loss of the lepton.

2.3 Polarization of Strange Hadrons in Quark Fragmentation

We now discuss in more detail how strange hadrons produced in the fragmentation of a polarized quark could also be polarized. The polarization of Λ^0 hyperons produced promptly or via a strange baryon Y in quark fragmenta-

tion is related to the quark polarization P_q , see Table 2, by:

$$P_{\Lambda^0}^q(Y) = -C_q^{\Lambda^0}(Y)P_q, \quad (6)$$

where $C_q^{\Lambda^0}(Y)$ is the corresponding spin transfer coefficient. The negative sign in (6) appears because of the opposite polarizations of the *incoming* and *outgoing* quarks: see Fig. 1.

We use two different models to calculate $C_q^{\Lambda^0}(Y)$. The first one is based on non-relativistic $SU(6)$ wave functions, where the Λ^0 spin is carried only by its constituent s quark. In this case, the promptly-produced Λ^0 hyperons could be polarized only in s quark fragmentation. However, Λ^0 hyperons produced via the decays of heavier strange hyperons originating from u or d quark fragmentation could also be polarized.

The second approach was suggested by Burkardt and Jaffe [22], who assumed that the ‘spin crisis’ exists not only for the nucleon, but also for other octet hyperons. Then, using flavor $SU(3)$ symmetry and polarized DIS data, they concluded that the u and d quarks inside the Λ^0 hyperon are polarized in the opposite direction to the Λ^0 spin at the level of -20% each. In the same way, the spin contents of all octet baryons were obtained in [27]. Then, they assumed that the polarized quark-to-hyperon fragmentation function was equal to the quark distribution function in that hyperon. We note that, in this Burkardt-Jaffe (BJ) model, all the strong-interaction effects are in principle included in the fragmentation and distribution functions. Therefore, one should not consider spin transfer from Σ^*

hyperons to the Λ^0 hyperon in BJ model. Table 3 summarizes the spin correlation coefficients in the $SU(6)$ and BJ models for both prompt Λ^0 hyperons and octet and decuplet intermediate hyperons.

2.4 Fragmentation Models

In order to apply our formalism to a real experimental environment, it is important to know the relative fractions of Λ^0 hyperons produced in different channels in both quark and diquark fragmentation in different regions of the DIS phase space.

It is well known from inclusive reactions at high energies that the typical hadronic rapidity correlation length is $\Delta y_h \simeq 2$. Thus to select, for example, the current fragmentation region one has to choose the hadrons with centre-of-mass rapidity $y_h^{CM} > 2$ [32]. According to this criterion, the minimal fraction z_{min} of the energy transferred to the struck quark required to select particles produced in the quark fragmentation region depends on the particle species and on the invariant mass of hadronic system, W . For example [33], in the case of Λ^0 production at $W = 5$ GeV, $\Delta y_h < 1.5$ at any value of z , and at $W = 20$ GeV the criterion is satisfied only for $z > 0.5$, where the production yield of Λ^0 hyperons is strongly suppressed.

However, as we now show, the beam energies in current experiments on Λ^0 polarization [7, 15, 16, 20, 21] are not enough for the $x_F > 0$ region to be populated by $q \rightarrow \Lambda^0$ fragmentation only.

To describe Λ^0 production and polarization in the full x_F interval, we use the LUND string fragmentation model,

as incorporated into the **JETSET7.4** program [34]. We use the **LEPTO6.5.1** [35] Monte Carlo event generator to simulate charged-lepton and (anti)neutrino DIS processes. With suitable choices of input parameters, these event generators reproduce well the distributions of various observables and particle yields. It was recently found by the NOMAD Collaboration that **JETSET7.4** with its default set of parameters overestimates the observable yields of strange hadrons produced in neutrino charged-current interactions by factors of 1.5 to 3 [36]. Therefore, we use here the new set of **JETSET** parameters found by the NOMAD Collaboration [37], so as to adjust the yields of strange particles in DIS processes. We have also modified the **LEPTO** code as follows:

- The cut on the minimal value of the energy in a fragmenting jet is removed. This was found by the NOMAD Collaboration to reproduce better the observed W^2 distribution in neutrino charged-current events.
- A split of the nucleon is implemented when the exchanged boson interacts with a sea u or d quark. In the default version of the **LEPTO** code, this is done for all sea quarks except u and d sea quarks.

In the framework of **JETSET**, it is possible to trace the particles' parentage. We use this information to check the origins of the strange hyperons produced in different kinematic domains, especially at various x_F . It is widely assumed that the current fragmentation region, defined to have $x_F > 0$, corresponds to the quark fragmentation region. However, as we mentioned above, arguing on the basis of the criterion [32], this is not true at moderate

energies, even for high z Λ^0 hyperons. According to the **LEPTO** and **JETSET** event generators, the x_F distribution of the diquark to Λ^0 fragmentation is weighted towards large negative x_F . However, its tail in the $x_F > 0$ region overwhelms the quark to Λ^0 x_F distribution at these beam energies. In Fig. 2, we show the x_F distributions of Λ^0 hyperons produced in diquark and quark fragmentation, as well as the final x_F distributions. We tag Λ^0 hyperons as being produced by quark and diquark fragmentation according to the rank of these particles in two different descriptions called ‘model A’ and ‘model B’, which we explain in Section 2.5. The distributions in Fig. 2 are shown for ν_μ CC DIS at the NOMAD mean neutrino energy $E_\nu = 43.8$ GeV, and for μ^+ DIS at the COMPASS muon beam energy $E_\mu = 160$ GeV. The relatively small fraction of the Λ^0 hyperons produced by quark fragmentation in the region $x_F > 0$ is related to the relatively small centre-of-mass energies - about 3.6 GeV for HERMES, about 4.5 GeV for NOMAD, about 8.7 GeV for COMPASS, and about 15 GeV for the E665 experiment - which correspond to low W . The authors [25], using on Lund and **JETSET** generators, also reported that the mean W^2 in HERMES and NOMAD is too low to populate the $x_F > 0$ region with struck-quark fragmentation alone.

The situation changes drastically for (anti)neutrino experiments, if the beam energy is increased to 500 GeV. As one can see in the left part of Fig. 3, now the $x_F > 0$ region is populated mainly by Λ^0 hyperons produced in quark fragmentation. However, the beam energy would have to be further doubled in the charged-lepton DIS process, in

order to populate the $x_F > 0$ region by struck-quark fragmentation. This is related to the lower $\langle W \rangle$ for electromagnetic interactions compared to that in (anti)neutrino DIS at the same beam energies.

2.5 Fixing Free Parameters of the Model.

We now compute the Λ polarization produced in any allowed kinematic domain, taking into account the Λ origins predicted by the LUND model, using the formalism developed in Sections 2.2 and 2.3. We assume that Λ^0 hyperons could be polarized only if they have one of the following origins:

1. Prompt Λ^0 hyperons containing the struck quark,
2. Λ^0 hyperons produced in the decays of heavier strange hyperons containing the struck quark,
3. Prompt Λ^0 hyperons containing the target nucleon remnant,
4. Λ^0 hyperons produced in the decays of heavier strange hyperons containing the remnant diquark.

In the framework of the JETSET generator, it is possible to identify Λ^0 hyperons unambiguously in one of these categories, since all hadrons generated in the Lund colour-string fragmentation model are ordered in rank from one end of the string to the other. Therefore, we introduce two rank counters: R_{qq} and R_q which correspond to the particle rank from the diquark and quark ends of the string, correspondingly. A hadron with $R_{qq} = 1$ or $R_q = 1$ would contain the diquark or the quark from one of the ends of the string.

However, one should perhaps not rely too heavily on the tagging specified in the LUND model. Therefore, we consider the following two variant fragmentation models:

Model A:

- The hyperon contains the stuck quark only if $R_q = 1$, and
- The hyperon contains the remnant diquark only if $R_{qq} = 1$.

Model B:

- The hyperon contains the stuck quark if $R_q \geq 1$ and $R_{qq} \neq 1$, and
- The hyperon contains the remnant diquark if $R_{qq} \geq 1$ and $R_q \neq 1$.

Clearly, Model B weakens the Lund tagging criterion by averaging over the string, whilst retaining information on the end of the string where the hadron originated.

We vary the two correlation coefficients $C_{sq_{val}}$ and $C_{sq_{sea}}$ in fitting Models A and B to the NOMAD Λ polarization data [15]. Scattering of the exchange W boson on the sea quark is expected to be enhanced in Λ^0 hyperons produced at low x_{Bj} or high W^2 . A strong target nucleon effect was also found by NOMAD. Therefore, we fit the following 4 NOMAD points to determine our free parameters:

- νp : $P_x^A = -0.26 \pm 0.05(stat)$,
- νn : $P_x^A = -0.09 \pm 0.04(stat)$,
- $W^2 < 15 \text{ GeV}^2$: $P_x^A(W^2 < 15) = -0.34 \pm 0.06(stat)$,
- $W^2 > 15 \text{ GeV}^2$: $P_x^A(W^2 > 15) = -0.06 \pm 0.04(stat)$.

We find from these fits similar values for both the $SU(6)$ and BJ models:

Model A: $C_{sq_{val}} = -0.35 \pm 0.05$, $C_{sq_{sea}} = -0.95 \pm 0.05$.

Model B: $C_{sq_{val}} = -0.25 \pm 0.05$, $C_{sq_{sea}} = 0.15 \pm 0.05$.

The error bars are obtained from the variation in the χ^2 functional around its minimum.

The coefficients found in models A and B are quite different, as could be anticipated from the different descriptions of the strange hadrons' origins in these models. However, the two fragmentation models give similar predictions for the polarization of Λ^0 hyperons produced in various lepton-nucleon DIS experiments, as we discuss in the next Section.

3 Results and Discussion

We present in this Section our model predictions for the longitudinal polarization of Λ^0 hyperons as a function of the kinematic variables W^2 , Q^2 , x_{Bj} , y_{Bj} , x_F and z in both charged- and neutral-current DIS for neutrinos and antineutrinos, and in charged-lepton DIS processes. Where data are available, we compare them with our model predictions.

3.1 Λ Polarization in (Anti)Neutrino DIS

3.1.1 Charged Currents

Our model predictions for the polarization of Λ hyperons produced in ν_μ charged-current DIS interactions off nuclei

as functions of different kinematic variables are shown in Fig. 4. The predictions are compared with the observed dependences of the Λ^0 polarization found by the NOMAD Collaboration [15, 17]. We see that the predictions of models A and B are both in quite good agreement with the NOMAD data, with model B perhaps being slightly preferred by the W^2 and x_{Bj} distributions. We note that Λ^0 polarization in quark fragmentation is calculated using the $SU(6)$ model for the spin transfer - see Table 3. However, as mentioned in Section 2.4, the fraction of Λ^0 hyperons produced via quark fragmentation is relatively small even at $x_F > 0$. Thus the predictions of the $SU(6)$ and BJ [22] spin-transfer models for the polarization of Λ^0 hyperons are indistinguishable within the experimental errors, at the present energies of DIS on fixed targets, and both models predict correctly the sign of Λ^0 polarization.

The NOMAD Collaboration has measured separately the polarization of Λ^0 hyperons produced off proton and neutron targets. Our model predictions are compared to the NOMAD data in Table 4. We observe good agreement, within the statistical errors, between the model B description and the NOMAD data. On the other hand, although model A reproduces quite well the polarization of Λ^0 hyperons produced from an isoscalar target, it does not describe so well the separate proton and neutron data.

The predictions for $\bar{\nu}_\mu$ charged-current DIS are shown in Fig. 5, for which data are currently not available. The neutrino energy was taken to be $E_\nu = 43.8$ GeV, which corresponds to the mean neutrino energy in the NOMAD experiment for events containing identified Λ^0 hyperons.

The predicted dependence on the target nucleon is summarized in Table 5.

3.1.2 Neutral Currents

The degree of Λ^0 polarization in (anti)neutrino neutral-current DIS processes is of great interest, since the Z^0 boson interacts with both flavours of valence quark, in contrast to charged-current interactions. Therefore, it is possible in principle to check the universality of C_{sq} coefficients using neutral-current data. We have been informed that the NOMAD Collaboration plans to investigate for the first time the polarization of Λ^0 and $\bar{\Lambda}^0$ hyperons produced in neutrino neutral-current DIS. Also, we observe that this process is of potential interest for a future neutrino factory [9].

Therefore, we provide here our model predictions for the polarization of Λ hyperons as a function of W^2 , Q^2 , x_{Bj} , y_{Bj} , x_F and z produced in the neutral-current DIS interactions with nuclei of neutrinos, in Figs. 6, and antineutrinos, in Figs. 7. In Tables 6 and 7 we summarize our model predictions for the target nucleon effects for ν_μ and $\bar{\nu}_\mu$ NC DIS processes respectively. The beam energy is again taken to be 43.8 GeV.

3.2 Λ Polarization and Spin Transfer in Charged-Lepton-Nucleon DIS

The sign of the polarization of Λ hyperons produced in polarized charged-lepton DIS off and unpolarized nucleon depends on the sign of the beam polarization. Therefore

we provide our model predictions for the spin transfer, which is defined as $P_A/P_B D(y)$. We note that the spin transfer is positive for negatively-polarized Λ^0 hyperons produced in the scattering of negatively-polarized beams.

3.2.1 HERMES

The HERMES experiment at HERA is collecting data on the polarization of Λ^0 hyperons produced in polarized e^+ beam interactions with different targets, including protons and neon nuclei [20]. We present here our model predictions for the spin transfer of Λ^0 hyperons, imposing the kinematic criteria used by HERMES Collaboration. The spin transfer as a function of kinematic variables predicted by our model is compared with the available HERMES data in Fig. 8. The observed x_F and z dependences of the Λ^0 spin transfer are compatible with our predictions. An investigation of the dependences of the Λ^0 polarization on other kinematic variables could be an important check of our model. More statistics would be needed to make a detailed comparison, and these may soon be provided by the new runs of HERA.

3.2.2 E665

The E665 Collaboration has reported [21] a measurement of the spin transfer to Λ^0 and $\bar{\Lambda}^0$ hyperons produced by the electromagnetic DIS of 470 GeV μ^+ . The kinematic domain used for the measurement was: $x_{Bj} < 0.1, 0.25 \text{ GeV}^2 < Q^2 < 2.5 \text{ GeV}^2$. In Fig. 9 we present our model predictions for the spin transfer to Λ hyperons produced in μ^+ DIS

interactions on nuclei in this kinematic domain. Unfortunately, the large experimental errors render the comparison with our model predictions inconclusive.

3.2.3 COMPASS

The COMPASS Collaboration plans to investigate the polarization of Λ^0 hyperons produced in the DIS of polarized μ^+ on a 6LiD target. The beam energy and polarization are 160 GeV and -0.8, respectively.

The calculated value of the spin transfer for events with $Q^2 > 1$ GeV 2 is presented as a function of different kinematic variables in Fig. 10. Thanks to the large statistics expected in this experiment, one can select kinematic regions where the predicted polarization is very sensitive to the value of the spin correlation coefficient for sea quarks, $C_{sq_{sea}}$. For example, in the region $x_F > -0.2$, which is experimentally accessible, and imposing the cut $0.5 < y < 0.9$, one ensure a large spin transfer from the incident lepton to the struck quark, and enhance the contribution from the sea quarks. The predicted Λ polarization is presented in Table 10.

4 Summary

We now summarize the key points of this paper. We have developed a model for Λ polarization in DIS that combines polarized intrinsic strangeness with non-relativistic $SU(6)$ wave functions. This model has been combined with the Lund model to describe the fragmentation processes. We have emphasized that the struck-quark and target frag-

mentation regions overlap significantly in experiments in the energy range currently available, and this effect is taken into account in our calculations.

Our model has only two free parameters, which are fixed from a fit to NOMAD data on the longitudinal polarization of Λ^0 hyperons produced in neutrino DIS. Our model describes well the various data available from this experiment [15, 17] and from experiments on charged-lepton DIS [20, 21]. We have proposed two model variants that differ in the extent to which Lund tagging information is used, and variant B is favoured by NOMAD data in which DIS off proton and neutron targets are separated. We have presented predictions for future data, including neutral-current DIS from NOMAD and charged-lepton DIS from HERMES and COMPASS. The dependences on the model details predicted here provide many possibilities for further checks of our approach.

We are grateful to G. Ingelman and T. Sjöstrand for useful discussions of the **LEPTO** and **JETSET** event generators. We thank A. V. Efremov, M. G. Sapozhnikov, R. Jaffe, Zuo-tang Liang and O. Teryaev for very interesting and valuable discussions. D. N. is grateful to all members of the NOMAD Collaboration, with special thanks to his Dubna collaborators in the Λ^0 polarization analysis: S. A. Bunyatov, A. V. Chukanov, D. V. Kustov and B. A. Popov. D. N. thanks also V. A. Naumov for valuable discussions of preliminary versions of this paper.

A - $SU(6)$ Wave Functions of Octet and Decuplet Hyperons

The quark-diquark $SU(6)$ wave functions of octet and decuplet baryons for non-vanishing matrix elements in (4) read:

$$\begin{aligned}
 A^\uparrow &= \frac{1}{\sqrt{12}}[2(ud)_{0,0}s^\uparrow + \sqrt{2}(us)_{1,1}d^\downarrow - \\
 &\quad -((us)_{1,0} - (us)_{0,0})d^\uparrow - \sqrt{2}(ds)_{1,1}u^\downarrow \\
 &\quad +((ds)_{1,0} - (ds)_{0,0})u^\uparrow], \\
 \Sigma^{0\uparrow} &= \frac{1}{\sqrt{18}}[2(ud)_{1,1}s^\downarrow - \sqrt{2}(ud)_{1,0}s^\uparrow + \\
 &\quad +\frac{1}{\sqrt{2}}((ds)_{1,0} + 3(ds)_{0,0})u^\uparrow - (ds)_{1,1}u^\downarrow + \\
 &\quad +\frac{1}{\sqrt{2}}((us)_{1,0} - 3(us)_{0,0})d^\uparrow - (us)_{1,1}d^\downarrow], \\
 \Sigma^{*+}{}^\uparrow &= \frac{1}{\sqrt{3}}[\sqrt{2}(us)_{1,1}u^\uparrow + (uu)_{1,1}s^\uparrow] \\
 \Sigma^{*+}{}^\uparrow &= \frac{1}{\sqrt{9}}[2(us)_{1,0}u^\uparrow + \sqrt{2}(us)_{1,1}u^\downarrow + \sqrt{2}(uu)_{1,0}s^\uparrow + \\
 &\quad +(uu)_{1,1}s^\downarrow] \\
 \Sigma^{*0}{}^\uparrow &= \frac{1}{\sqrt{3}}[(ds)_{1,1}u^\uparrow + (ud)_{1,1}s^\uparrow + (us)_{1,1}d^\uparrow] \\
 \Sigma^{*0\uparrow} &= \frac{1}{\sqrt{18}}[2(ds)_{1,0}u^\uparrow + \sqrt{2}(ds)_{1,1}u^\downarrow + 2(us)_{1,0}d^\uparrow \\
 &\quad +\sqrt{2}(us)_{1,1}d^\downarrow + 2(ud)_{1,0}s^\uparrow + \sqrt{2}(ud)_{1,1}s^\downarrow], \tag{7}
 \end{aligned}$$

where $\Sigma^{*+}{}^\uparrow$ ($\Sigma^{*+}{}^\uparrow$) denotes a Σ^* state with $M = \frac{3}{2}$ ($M = \frac{1}{2}$). The symbols $(qq')_{J,M}$ represent the diquark in the spin state $|J, M\rangle$.

B - Details of P_Λ Calculations

We use non-relativistic $SU(6)$ wave functions (see App. A) in order to compute the matrix elements in (4). We consider here in more detail calculations for Λ hyperons pro-

duced in charged-lepton-nucleon, as the most general example. In this case, the struck quark can be polarized *only* if the beam or/and target are polarized. We consider the case of polarized beam and unpolarized target. After removing a polarized quark q from the nucleon, the product of the wave functions of the diquark remnant and s quark reads:

$$\begin{aligned}
 |N \ominus q_{pol}\rangle \otimes |s_{pol}\rangle &= \\
 \frac{1}{2} \left[\sqrt{1+P_q} |N \ominus q^\uparrow\rangle \left(\sqrt{1+C_{sq}}s^\uparrow + \sqrt{1-C_{sq}}s^\downarrow \right) + \right. \\
 \left. + \sqrt{1-P_q} |N \ominus q^\downarrow\rangle \left(\sqrt{1-C_{sq}}s^\uparrow + \sqrt{1+C_{sq}}s^\downarrow \right) \right],
 \end{aligned}$$

where $(\sqrt{1+C_{sq}}s^\uparrow + \sqrt{1-C_{sq}}s^\downarrow)$ corresponds to the spin part of the polarized s quark wave function, and $|N \ominus q_{pol}\rangle$ is the wave function of the nucleon remnant. Explicitly:

$$\begin{aligned}
 |p \ominus d^\uparrow\rangle &= \frac{1}{\sqrt{36}}[-\sqrt{2}(uu)_{1,0} + 2(uu)_{1,-1}], \\
 |p \ominus u^\uparrow\rangle &= \frac{1}{\sqrt{36}}[3(ud)_{0,0} + (ud)_{1,0} - \sqrt{2}(ud)_{1,-1}], \\
 |n \ominus d^\uparrow\rangle &= \frac{1}{\sqrt{36}}[3(ud)_{0,0} + (ud)_{1,0} - \sqrt{2}(ud)_{1,-1}], \\
 |n \ominus u^\uparrow\rangle &= \frac{1}{\sqrt{36}}[-\sqrt{2}(uu)_{1,0} + 2(uu)_{1,-1}]. \tag{8}
 \end{aligned}$$

Using (4, 7, 8), one can obtain the results presented in (5).

References

1. J. Ashman *et al.*, [EMC Collaboration], Phys. Lett. **B206**, 364 (1988);
Nucl. Phys. **B328** (1989) 1.

2. D. Adams *et al.*, [SMC Collaboration], Phys. Rev. **D56**, 5330 (1997);
- B. Adeva *et al.*, [SMC Collaboration], Phys. Lett. **B420**, 180 (1998).
3. K. Abe *et al.*, [E143 Collaboration], Phys. Rev. **D58**, 112003 (1998).
4. P. L. Anthony *et al.*, [SLAC E155 Collaboration], Phys. Lett. **B458**, 529 (1999).
5. K. Ackerstaff *et al.*, [HERMES Collaboration], Phys. Lett. **B464**, 123 (1999).
6. A. Efremov and O. Teryaev, JINR preprint, JINR-E2-88-287 (1988);
G. Altarelli and G. Ross, Phys. Lett. **B212** 391 (1988);
R. Carlitz, J. Collins and A. Mueller, Phys. Lett. **B214** 229 (1988).
7. The COMPASS Proposal, CERN/SPSLC 96-14, SPSC/P297, March 1996.
8. W. M. Alberico, S. M. Bilenky and C. Maierov, hep-ph/0102269.
9. M. L. Magnano *et al.*, CERN-TH/2001-131, hep-ph/0105155.
10. J. Ellis, M. Karliner, D. E. Kharzeev and M. G. Sapozhnikov, Phys. Lett. **B353** (1995) 3129; Nucl. Phys. **A673** 256 (2000).
11. J. Ellis, D. E. Kharzeev and A. Kotzinian, Z. Phys. **C69** 467 (1996).
12. J. T. Jones *et al.*, [WA21 Collaboration], Z. Phys. **C28** 23 (1987).
13. S. Willocq *et al.*, [WA59 Collaboration], Z. Phys. **C53** 207 (1992).
14. D. DeProspo *et al.*, [E632 Collaboration], Phys. Rev. **D50** 6691 (1994).
15. P. Astier *et al.*, [NOMAD Collaboration], Nucl. Phys. **B588** (2000) 3;
- D. V. Naumov [NOMAD Collaboration], AIP Conf. Proc. **570** (2001) 489, hep-ph/0101325.
16. P. Astier *et al.* [NOMAD Collaboration], Nucl. Phys. **B605**, 3 (2001) hep-ex/0103047.
17. D. V. Naumov, Ph.D. Thesis, JINR, Dubna, Russia, (2001), *in Russian*. (available upon request).
18. W. Melnitchouk and A. W. Thomas, Z. Phys. **A353** 311 (1996).
19. D. Buskulic *et al.* [ALEPH Collaboration], Phys. Lett. **B374**, 319 (1996);
K. Ackerstaff *et al.* [OPAL Collaboration], Eur. Phys. J. **C2**, 49 (1998), hep-ex/9708027.
20. A. Airapetian *et al.* [HERMES Collaboration], Phys. Rev. **B64**, 112005 (2001) hep-ex/9911017;
S. Belostotski, *IXth Workshop on High-Energy Spin Physics*, Dubna, Russia, Aug 2 - 7, 2001.
21. M. R. Adams *et al.* [E665 Collaboration], Eur. Phys. J. **C17**, 263 (2000), hep-ex/9911004.
22. M. Burkardt and R. L. Jaffe, Phys. Rev. Lett. **70**, 2537 (1993)
23. M. Anselmino, M. Boglione, U. D'Alesio and F. Murgia, hep-ph/0106256; M. Anselmino, M. Boglione, U. D'Alesio, E. Leader and F. Murgia, Phys. Lett. B **509**, 246 (2001), hep-ph/0102119; M. Anselmino, D. Boer, U. D'Alesio and F. Murgia, hep-ph/0010291; M. Boglione, M. Anselmino and F. Murgia, hep-ph/0010166; M. Anselmino, D. Boer, U. D'Alesio and F. Murgia, Phys. Rev. D **63**, 054029 (2001), hep-ph/0008186; M. Anselmino, M. Boglione and F. Murgia, Phys. Lett. B **481**, 253 (2000), hep-ph/0001307.

24. A. M. Kotzinian, hep-ph/9709259; A. M. Kotzinian, A. Bravar and D. von Harrach, Eur. Phys. J. **C2**, 329 (1998), hep-ph/9701384.

25. C. x. Liu, Q. h. Xu and Z. t. Liang, Phys. Rev. **D64**, 073004 (2001), hep-ph/0106184; Liang Zuo-tang, hep-ph/0111403; Liang Zuo-tang, talk given at the *3rd Circum Pan-Pacific Symposium on High-Energy Spin Physics*, October 2001, Beijing, China.

26. Z. t. Liang, hep-ph/9809593; Z. t. Liang, hep-ph/9809593; C. Boros, Z. t. Liang and T. c. Meng, hep-ph/9610487.

27. C. Boros and Z. t. Liang, Phys. Rev. **D57**, 4491 (1998), hep-ph/9803225.

28. J. J. Yang, hep-ph/0111382; J. J. Yang, Phys. Rev. **D64**, 074010 (2001), hep-ph/0111188; J. J. Yang, Phys. Lett. **B512**, 57 (2001), hep-ph/0107222; J. Soffer, Nucl. Phys. Proc. Suppl. **79**, 551 (1999); B. Q. Ma, I. Schmidt, J. Soffer and J. J. Yang, Phys. Lett. **B488**, 254 (2000), hep-ph/0005210; B. Q. Ma, I. Schmidt, J. Soffer and J. J. Yang, Eur. Phys. J. **C16**, 657 (2000), hep-ph/0001259; B. Q. Ma, I. Schmidt and J. J. Yang, Phys. Rev. **D61**, 034017 (2000), hep-ph/9907224; B. Q. Ma, I. Schmidt and J. J. Yang, Phys. Lett. **B477**, 107 (2000), hep-ph/9906424; B. Q. Ma and J. Soffer, Phys. Rev. Lett. **82**, 2250 (1999), hep-ph/9810517.

29. D. de Florian, M. Stratmann and W. Vogelsang, Phys. Rev. **D57**, 5811 (1998), hep-ph/9711387.

30. D. Ashery and H.J. Lipkin, Phys. Lett. **B469** 263 (1999).

31. I.I. Bigi, Nuovo. Cim. **41A** 43, *ibid.* 581 (1977).

32. E. Berger, preprint ANL-HEP-PR-87-45.

33. P. J. Mulders, hep-ph/0010199.

34. T. Sjöstrand, *PYTHIA 5.7 and JETSET 7.4: physics and manual*, LU-TP-95-20 (1995), hep-ph/9508391; T. Sjöstrand, Comp. Phys. Commun. **39** 347 (1986), **43** 367 (1987).

35. G. Ingelman, A. Edin and J. Rathsman, Comp. Phys. Commun. **101** 108 (1997).

36. P. Astier *et al.* [NOMAD Collaboration], Nucl. Phys. **B621**, 3 (2002), hep-ex/0111057; D. V. Naumov and B. A. Popov, JINR Report E1-2001-139 (2001).

37. P. Astier *et al.* [NOMAD Collaboration], *in preparation*; A. V. Chukanov, D. V. Naumov and B. A. Popov, NOMAD Internal Note 2001-04 (available upon request).

38. A. Kotzinian, *Second Workshop EPIC 2000*, Cambridge, Massachusetts 2000, AIP Conf. Proc. **V588**, 272 (2001).

39. S. J. Brodsky and B.-Q. Ma, Phys. Lett. **B381** 317 (1996).

40. C. Boros, J. T. Londergan and A. W. Thomas, Phys. Rev. **D61** (2000) 014007; *ibid* **D62** 014021 (2000).

41. M. A. Shifman, A. I. Vainshtein and V. I. Zakharov, Nucl. Phys. **B147** 385, 448, 519 (1979); B. L. Ioffe, Nucl. Phys. **B188** 317 [Erratum: **B191** 591 (1981)]; L. J. Reinders, H. Rubinshtein and S. Yazaki, Phys. Rep. **127** 1 (1985).

List of Figures

1	Polarization transfer to promptly-produced Λ^0 hyperons in νn charged-current DIS.	17	5	The predictions of model A - solid line and model B - dashed line, for the polarization of Λ hyperons produced in $\bar{\nu}_\mu$ charged-current DIS interactions off nuclei as functions of W^2 , Q^2 , x_{Bj} and y_{Bj}	18
2	Predictions for the x_F distributions of all Λ^0 hyperons (solid line), of those originating from diquark fragmentation and of those originating from quark fragmentation, for the two model variants A and B, as explained in the legend on the plots. The left panel is for ν_μ CC DIS with $E_\nu = 43.8$ GeV, and the right panel for μ^+ DIS with $E_\mu = 160$ GeV.	17	6	The predictions of model A - solid line, model B - dashed line, for the polarization of Λ hyperons produced in ν_μ neutral-current DIS interactions off nuclei as functions of W^2 , Q^2 , x_{Bj} , y_{Bj} , x_F and z (at $x_F > 0$).	19
3	Predictions for the x_F distribution of all Λ^0 hyperons (solid line), of those originating from diquark fragmentation and of those originating from quark fragmentation, for the two model variants A and B, as explained in the legend on the plots. The left panel is for ν_μ CC DIS with $E_\nu = 500$ GeV, and the right panel for μ^+ DIS with $E_\mu = 500$ GeV.	17	7	The predictions of model A - solid line, model B - dashed line, for the polarization of Λ hyperons produced in $\bar{\nu}_\mu$ neutral-current DIS interactions off nuclei as functions of W^2 , Q^2 , x_{Bj} , y_{Bj} , x_F and z (at $x_F > 0$).	19
4	The predictions of model A - solid line and model B - dashed line, for the polarization of Λ hyperons produced in ν_μ charged-current DIS interactions off nuclei as functions of W^2 , Q^2 , x_{Bj} , y_{Bj} , x_F and z (at $x_F > 0$). The points with error bars are from [15,17].	18	8	The predictions of model A - solid line, model B - dashed line, for the spin transfer to Λ hyperons produced in e^+ DIS interactions off nuclei as functions of W^2 , Q^2 , x_{Bj} , y_{Bj} , x_F and z (at $x_F > 0$). We assume $E_e = 27.5$ GeV, and the points with error bars are from [20].	20

9 The predictions of model A - solid line, model B - dashed line, for the spin transfer to Λ hyperons produced in μ^+ DIS interactions off nuclei as functions of W^2 , Q^2 , x_{Bj} , y_{Bj} , x_F and z (at $x_F > 0$). Here we assume $E_\mu = 470$ GeV, as appropriate for E665. 20

10 The predictions of model A - solid line, model B - dashed line, for the spin transfer to Λ hyperons produced in μ^+ DIS interactions off nuclei as functions of W^2 , Q^2 , x_{Bj} , y_{Bj} , x_F and z (at $x_F > 0$). here we assume $E_\mu = 160$ GeV, as appropriate for COMPASS. 21

List of Tables

1	<i>Longitudinal polarization of Λ^0 hyperons observed in bubble chamber (anti)neutrino experiments.</i>	21
2	<i>Polarization of the struck quark in different processes.</i>	21
3	<i>Spin correlation coefficients in the SU(6) and BJ models</i>	22
4	<i>Dependence of the polarization of Λ hyperons produced in ν_μ CC DIS on the type of target nucleon, compared with the NO-MAD [15] data.</i>	22
5	<i>Model predictions for the polarization of Λ hyperons produced in $\bar{\nu}_\mu$ CC DIS.</i>	22
6	<i>Model predictions for the polarization of Λ hyperons produced in ν_μ NC DIS.</i>	22
7	<i>Model predictions for the polarization of Λ hyperons produced in $\bar{\nu}_\mu$ NC DIS.</i>	22
8	<i>Model predictions for the polarization of Λ hyperons produced in e^+ DIS with the HERMES experiment.</i>	22
9	<i>Model predictions for the polarization of Λ hyperons produced in μ^+ DIS with the E665 experiment.</i>	22
10	<i>Model predictions for the polarization of Λ hyperons produced in μ^+ DIS with the COMPASS experiment, for $Q^2 > 1$ GeV2, $x_F > -0.2$ and $0.5 < y < 0.9$.</i>	23

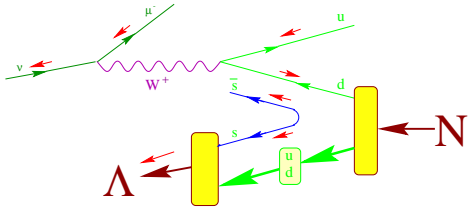


Fig. 1. Polarization transfer to promptly-produced Λ^0 hyperons in νn charged-current DIS.

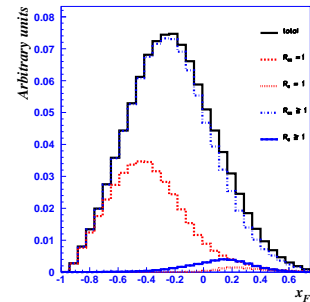


Fig. 2. Predictions for the x_F distributions of all Λ^0 hyperons (solid line), of those originating from diquark fragmentation and of those originating from quark fragmentation, for the two model variants A and B, as explained in the legend on the plots. The left panel is for ν_μ CC DIS with $E_\nu = 43.8$ GeV, and the right panel for μ^+ DIS with $E_\mu = 160$ GeV.

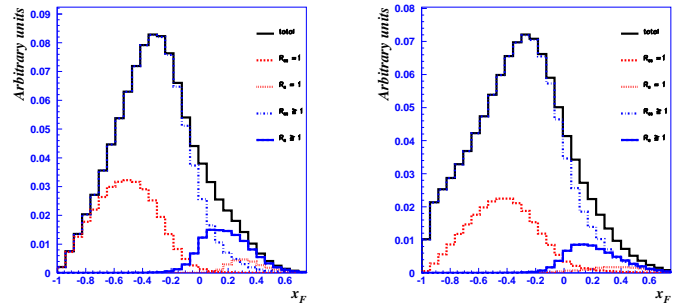


Fig. 3. Predictions for the x_F distribution of all Λ^0 hyperons (solid line), of those originating from diquark fragmentation and of those originating from quark fragmentation, for the two model variants A and B, as explained in the legend on the plots. The left panel is for ν_μ CC DIS with $E_\nu = 500$ GeV, and the right panel for μ^+ DIS with $E_\mu = 500$ GeV.

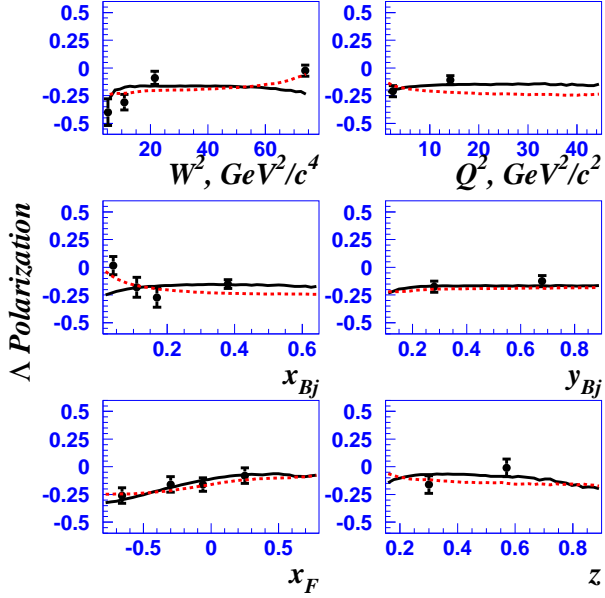


Fig. 4. The predictions of model A - solid line and model B - dashed line, for the polarization of Λ hyperons produced in ν_μ charged-current DIS interactions off nuclei as functions of W^2 , Q^2 , x_{Bj} , y_{Bj} , x_F and z (at $x_F > 0$). The points with error bars are from [15,17].

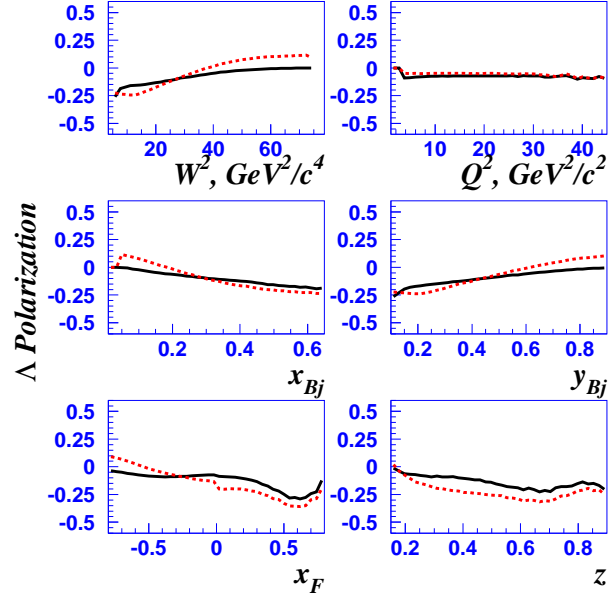


Fig. 5. The predictions of model A - solid line and model B - dashed line, for the polarization of Λ hyperons produced in $\bar{\nu}_\mu$ charged-current DIS interactions off nuclei as functions of W^2 , Q^2 , x_{Bj} and y_{Bj} .

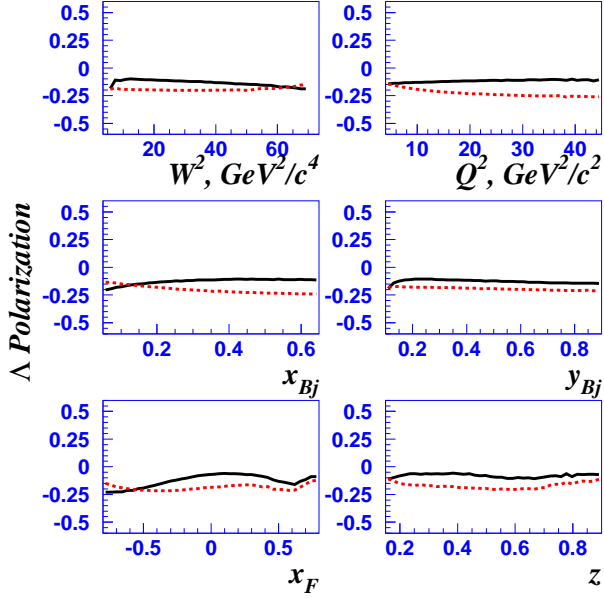


Fig. 6. The predictions of model A - solid line, model B - dashed line, for the polarization of Λ hyperons produced in ν_μ neutral-current DIS interactions off nuclei as functions of W^2 , Q^2 , x_{Bj} , y_{Bj} , x_F and z (at $x_F > 0$).

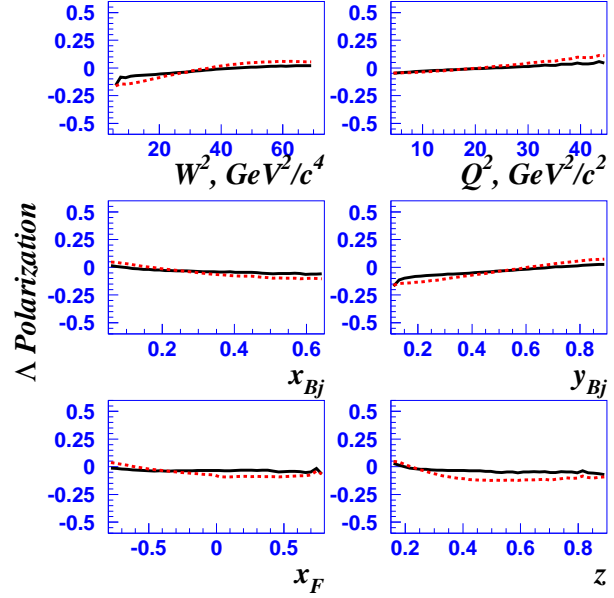


Fig. 7. The predictions of model A - solid line, model B - dashed line, for the polarization of Λ hyperons produced in $\bar{\nu}_\mu$ neutral-current DIS interactions off nuclei as functions of W^2 , Q^2 , x_{Bj} , y_{Bj} , x_F and z (at $x_F > 0$).

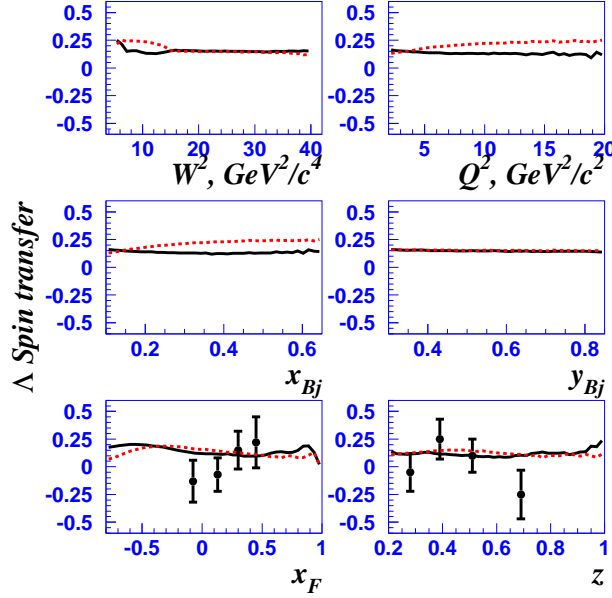


Fig. 8. The predictions of model A - solid line, model B - dashed line, for the spin transfer to Λ hyperons produced in e^+ DIS interactions off nuclei as functions of W^2 , Q^2 , x_{Bj} , y_{Bj} , x_F and z (at $x_F > 0$). We assume $E_e = 27.5$ GeV, and the points with error bars are from [20].

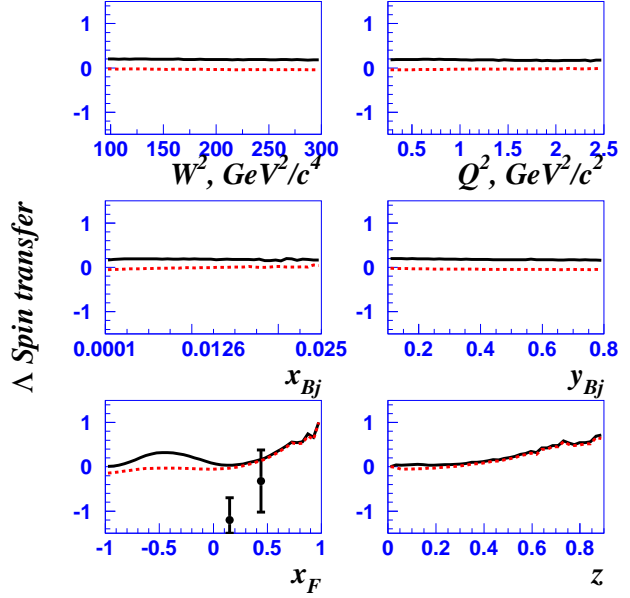


Fig. 9. The predictions of model A - solid line, model B - dashed line, for the spin transfer to Λ hyperons produced in μ^+ DIS interactions off nuclei as functions of W^2 , Q^2 , x_{Bj} , y_{Bj} , x_F and z (at $x_F > 0$). Here we assume $E_\mu = 470$ GeV, as appropriate for E665.

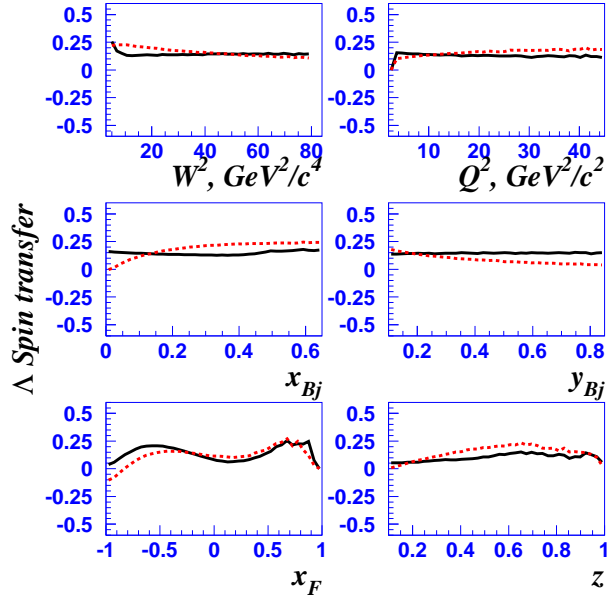


Fig. 10. The predictions of model A - solid line, model B - dashed line, for the spin transfer to Λ hyperons produced in μ^+ DIS interactions off nuclei as functions of W^2 , Q^2 , x_{Bj} , y_{Bj} , x_F and z (at $x_F > 0$). here we assume $E_\mu = 160$ GeV, as appropriate for COMPASS.

Table 1. Longitudinal polarization of Λ^0 hyperons observed in bubble chamber (anti)neutrino experiments.

Process Exp.(Year)	$\langle E_\nu \rangle$ [GeV]	cut on x_F	N_{Λ^0}	P_x
$\nu_\mu - p$ WA21 [12](1985)	51	Full sample	289	-0.10 ± 0.14
		$x_F < 0$	203	-0.29 ± 0.18
	40	$x_F > 0$	86	0.53 ± 0.30
		Full sample	267	-0.24 ± 0.17
$\bar{\nu}_\mu - p$ WA59 [13](1992)	40	$x_F < 0$	210	-0.38 ± 0.18
		$x_F > 0$	57	0.32 ± 0.35
	40	Full sample	469	-0.56 ± 0.13
		$x_F < 0$	403	-0.63 ± 0.13
$\nu_\mu - Ne$ WA59 [13](1992)	150	$x_F > 0$	66	-0.11 ± 0.45
		Full sample	258	-0.38 ± 0.16
E632 [14]		$x_F < 0$	190	-0.43 ± 0.20

Table 2. Polarization of the struck quark in different processes.

	ν		$\bar{\nu}$		l^\pm
	CC	NC	CC	NC	γ
P_d	1	$\frac{(1-\xi)^2 - \xi^2(1-y)^2}{(1-\xi)^2 + \xi^2(1-y)^2}$	—	$\frac{(1-\xi)^2(1-y)^2 - \xi^2}{(1-\xi)^2(1-y)^2 + \xi^2}$	$P_B D(y)$
P_u	—	$\frac{(1-2\xi)^2 - 4\xi^2(1-y)^2}{(1-2\xi)^2 + 4\xi^2(1-y)^2}$	1	$\frac{(1-2\xi)^2(1-y)^2 - 4\xi^2}{(1-2\xi)^2(1-y)^2 + 4\xi^2}$	$P_B D(y)$

Table 3. Spin correlation coefficients in the $SU(6)$ and BJ models

Λ^0 's parent	$C_u^{\Lambda^0}$		$C_d^{\Lambda^0}$		$C_s^{\Lambda^0}$	
quark	SU(6)	BJ	SU(6)	BJ	SU(6)	BJ
	0	-0.18	0	-0.18	1	0.63
Σ^0	-2/9	-0.12	-2/9	-0.12	1/9	0.15
Ξ^0	-0.15	0.07	0	0.05	0.6	-0.37
Ξ^-	0	0.05	-0.15	0.07	0.6	-0.37
Σ^*	5/9	-	5/9	-	5/9	-

Table 4. Dependence of the polarization of Λ hyperons produced in ν_μ CC DIS on the type of target nucleon, compared with the NOMAD [15] data.

P_A (%)	Target nucleon		
	isoscalar	proton	neutron
model A	-17.4	-11.4	-20.2
model B	-19.3	-18.1	-19.9
NOMAD	-15.0 ± 3	-26.0 ± 5	-9.0 ± 4

Table 5. Model predictions for the polarization of Λ hyperons produced in $\bar{\nu}_\mu$ CC DIS.

P_A (%)	Target nucleon		
	isoscalar	proton	neutron
model A	-7.9	-10.7	-3.4
model B	-5.0	-6.7	-2.3

Table 6. Model predictions for the polarization of Λ hyperons produced in ν_μ NC DIS.

P_A (%)	Target nucleon		
	isoscalar	proton	neutron
model A	-12.9	-11.7	-13.9
model B	-19.6	-19.6	-19.7

Table 7. Model predictions for the polarization of Λ hyperons produced in $\bar{\nu}_\mu$ NC DIS.

P_A (%)	Target nucleon		
	isoscalar	proton	neutron
model A	-3.0	-1.8	-4.3
model B	-3.1	-2.8	-3.4

Table 8. Model predictions for the polarization of Λ hyperons produced in e^+ DIS with the HERMES experiment.

P_A (%)	Target nucleon		
	isoscalar	proton	neutron
model A	-4.1	-4.6	-3.5
model B	-4.3	-4.4	-4.1

Table 9. Model predictions for the polarization of Λ hyperons produced in μ^+ DIS with the E665 experiment.

P_A (%)	Target nucleon		
	isoscalar	proton	neutron
model A	-4.7	-4.7	-4.7
model B	1.1	1.0	1.2

Table 10. *Model predictions for the polarization of Λ hyperons*produced in μ^+ DIS with the COMPASS experiment, for $Q^2 >$ 1 GeV^2 , $x_F > -0.2$ and $0.5 < y < 0.9$.

P_Λ (%)	Target nucleon		
	isoscalar	proton	neutron
model A	-6.3	-6.1	-6.6
model B	-3.0	-3.1	-2.8